Effect of Variable Viscosity and Activation Energy on Convective Heat and Mass Transfer Flow of Nanofluid Past a Vertical Wavy with Thermal Radiation and Chemical Reaction in the Presence of Heat Generating Sources

Dr. Y. Madhusudhana Reddy
Associate Professor, Department of Mathematics,
Sri Venkateswara Institute of Technology, Anantapuramu, A.P., India

Article Info
Page Number: 249 – 272
Publication Issue:
Vol 68 No. 1 (2019)

Abstract
We investigate effect of variable viscosity, activation energy on natural convective heat and mass transfer flow over a vertical wavy surface embedded in a fluid saturated porous medium with thermal radiation. The vertical wavy wall and the governing equations for flow heat ad mass transfer are transformed to a plane geometry case by employing the Runge-Kutta fourth order with Shooting technique. The non-dimensional velocity, temperature and nano-concentration graphs as well as skin friction, rate of heat and mass transfer coefficients are displayed for different values of variable viscosity, activation energy, radiation parameter, heat source parameter, chemical reaction and amplitude of the wavy surface. It is found that the increase in variable viscosity increases the velocities, reduces the temperature .The concentration reduces in the region adjacent to the wall and enhances far away from the wall, velocities, temperature and concentration experience enhancement with activation energy parameter.

Article History
Article Received: *09 September 2019*
Revised: *16 October 2019*
Accepted: *21 November 2019*
Publication: *28 December 2019*

Keywords: - Nano fluid, Wavy Wall, variable viscosity, activation energy, Thermal Radiation, Chemical reaction, Heat Sources

1.Introduction:

Study of convective heat transfer in nanofluids has become a topic of contemporaneous interest due to its applications in several industries such as power plant operations, manufacturing and transportation, electronics cooling, heat exchangers. The word “nanofluid” coined by Choi [13] refers to a liquid suspension containing ultra - fine particles (diameter less than 50 nm). The traditional fluids used for heat transfer applications such as water, mineral oils, ethylene glycol, engine oil have limited heat transfer capabilities. The nanofluids which are the engineered colloidal suspension of nano meter sized particle of metals and metallic oxides such as aluminum, copper, gold, iron and titanium or their oxides in base fluids. The base fluids are usually water, oil, ethylene glycol, bio fluids and toluene. Experimental investigations revealed that base fluids with suspension of the nanoparticles have substantially higher thermal conductivities than those of the base fluids. Eastman et al. [18] and Minsta [48] showed that even with small volumetric fraction of nanoparticles (less than 5%), the thermal conductivity of the base liquid can be enhanced by 10 - 50%. It was reported that a small amount (less than 1% volume fraction) of copper nanoparticles or carbon nanotubes dispersed in ethylene glycol or oil can increase their inherently poor

thermal conductivity by 40% and 50%, respectively (Eastman et al., [18]; Choi et al., [13]. The unique properties of these nanofluids made them potential to use in many applications in heat transfer. A recent application of the nanofluid as suggested by Kleinstreuer et al.,[39] is in delivery of nano-drug. Eastman et al., [17] attributed the enhancement of thermal conductivity to the increase in surface area due to the suspension of nanoparticles. Keblinski et al., [35] discussed on the possible mechanisms for the improved thermal conductivity. According to them the contribution of Brownian motion is much less than other factors such as size effect, clustering of nanoparticles and surface adsorption. Buongiorno [11] evaluated the different theories explaining the enhanced heat transfer characteristics of nanofluids. He developed an analytical model for convective transport in nanofluids which takes into account the Brownian diffusion and thermophoresis. Using this model, Kuznetsov and Nield [40] investigated the natural convective flow of a nanofluid over a vertical plate. Effect of magnetic fuel on free convection flow of a nanofluid past a vertical semi-infinite flat plate has been discussed by Hamad et al. [18]. Gorla and Chamkha [25] investigated natural convection flow past a horizontal plate in a porous medium filled with a nanofluid. The fluid flow due to a stretching surface has important applications such as production of glass and paper sheets, metal spinning, hot rolling, drawing of plastic films, and extrusion of metals and polymers. Khan and Pop [38] studied the boundary layer flow of a nanofluid past a stretching sheet. The heat and mass transfer analysis for boundary layer stagnation – point flow over a stretching sheet in a porous medium saturated by a nanofluid with internal heat generation/absorption and suction/blowing is investigated by Hamad and Ferdows [26]. Nadeem and Lee [50] made an analytical investigation of the problem of steady boundary layer flow of a nanofluid over an exponential stretching surface including the effects of Brownian motion and thermophoresis. Makinde and Aziz [44] studied the boundary layer flow of a nanofluid past a stretching sheet with a convective boundary condition. Rana and Bhargava [52] analyzed numerically the flow and heat transfer of a nanofluid over a nonlinearly stretching sheet.

The study of magnetohydrodynamics has significant applications in engineering. MHD generators, devices in petroleum industry, material processing, nuclear reactors etc are some applications. The use of magnetic fields plays an important role in the process of purification of molten metals from non metallic inclusions. Several authors (Abd El-Aziz [1], Abo-Eldahab and Abd El-Aziz [2], Abo-Eldahab and Salem [3], Ali et al. [4]) have demonstrated the effect of magnetic field on mixed convective heat transfer flow of nanofluid in different configurations. Xiaohonh Su and Liancun Zheng [72] studied the Hall effect on MHD flow and heat transfer of nanofluids over a stretching wedge in the presence of velocity slip and Joule heating. Four different types of water-based nanofluids containing copper (Cu), silver (Ag), alumina (Al_2O_3), and titania (TiO_2) nanoparticles are investigated. Mohamed Abd El-Aziz [49] analyzed the effects of Hall current on the steady boundary layer MHD slip flow over a stretching sheet in a water-based nanofluid containing different types of nanoparticles: Cu, Al_2O_3 and Ag.

In recent years energy and material saving considerations have prompted an expansion of the efforts at producing efficient heat exchanger equipment through augmentation of heat transfer. Hence it is advantageous to go for converging-diverging geometries for improving the design of heat transfer equipment. Several researchers

(Deshikachar et al [14], Goren[23], Leela Kumari et.al. [42], Rao *et. al.* [53], Rees & Pop [54], Sree Ramachandra Murthy [62], Vajravelu and Debnath [65], Vajravelu and Nayfeh [66], Vajravelu and Sastry [67],). The influence of a variable heat flux on natural convection along a corrugated wall in a non-Darcy porous medium was established by Shalini and Kumar [57]. Ching-Yang Cheng [12] have discussed the double diffusive natural convection along an inclined wavy surface in a porous medium Manjulatha [46] have discussed heat and mass transfer effects in a viscous incompressible fluid through a porous medium confined between a long vertical wavy wall and a parallel flat wall in an aligned magnetic field.

The study of heat generation or absorption effects in moving fluids is important in view of several physical problems such as fluids undergoing exothermic or endothermic chemical reactions. The volumetric heat generation has been assumed to be constant or a function of space variable. For example a hypothetical core – disruptive accident in a liquid metal fast breeder reactor (LMFBR) could result in the setting of fragmented fuel debris on horizontal surfaces below the core. The porous debris could be saturated sodium coolant and heat generation will result from the radioactive decay of the fuel particulate. Vajravelu and Hadjinicolaou [69], Hossain et al [29], Mallikarjuna [45], Ramakrishna and Satyanarayana [51] have discussed the effect of heat sources on convective heat and mass transfer flow past a wavy wall.

In most of the studies, the viscosity of the fluid was assumed to be constant. When the effects of variable viscosity is taken into account, the flow characteristics are significantly changed compared to the constant property case.Convection flow in nature and engineering phenomena requires that viscosity and thermal conductivity of fluids vary with temperature.For instance,the viscosityof dry air at 100^0 C is $21.94x10^{-6}$ kg/ms while at 200^0 C.it is $26.94x10^{-6}$ kg/ms. Dulal and Hiramony [16] analysed the effects of temperature-dependent viscosity and variable thermal conductivity on mixed convective diffusion flow. They found that velocity profile increases while temperature decreases with increase in mixed convection. Vajravelu et al [68], Singh and Shweta [60] and Isaac and Anselm [32] shoed that, velocity distribution decreases with increase in viscositywhile the temperature profiles increase with increase in variable viscosity. Devi and Prakash [15] examined temperature-dependent viscosity and thermal conductivity effects on hydromagnetic flow over a slandering stretchinmg sheet. They concluded that ,increase in viscosity decreases the velocity profiles. The work of Animasaun [6] concluded that the fluid velocity decreases wihile temperature increases with increasing viscosity. The works of Gopal and Jadav [22], Jadav and Hazarika [33], Gopal and Banditya [21], Bandita [8], Kareem and Salawu [34] have shown that the velocity profiles decrease with increasing viscosity while tyemperature profiles decrease with increase in viscosity. Sreenivasulu et al [61] studied variable thermal conductivity by influence on hydromagnetic flow past a stretching cylinder in a thermally swtratified medium with heat source/sink. Makinde et al. [43] describes the MHD flow of a variable viscosity nanofluid over a radially stretching convective surface with radiative heat. Mallikarjuna [45] have discussed the effect of variable viscosity and thermal conductivity on convective heat and mass transfer flow over a vertical wavy surface in a porous medium with variable properties. Recently, Srinivasa Reddy et al [64] have demonstrated the effect of radiation, chemical reaction, heat sources, wavy surface on the flow past a wavy wall.

The chemical reaction is more efficient (maximizing the yield) if the number of reagents, energy inputs, and wastage are minimized. In a reaction, all the particles can have either potential energy or kinetic energy. The activation energy (AE) is defined as the minimum energy required for the chemical reaction to occur. The concept of AE is essentially helpful in the manufacturing industry, geothermal and oil res ervoir engineering fields, chemical engineering, food processing units, and so forth. Ijaz et al [31] analyzed the effects of AE on magnetohydrodynam ic (MHD) radiative flow of non-Newtonian fluid on a rotating disk. The study concludes that the concentration of the rheological fluid decreases with rising Schmidt number and reverses behavior with the AE parameter. Khan et al [37] discussed the nonlinear radiative nanofluid flow along the streamwise direction in the presence of AE. They observed that multiple outputs are obtained for moving parameters and the rate of heat transfer diminishes with rising thermal heat parameters. Azama et al [7] examined numerically the influence of Arrhenius AE on the axisymmetric flow of a nanofluid through the Brownian diffusion mechanism. They found that the therma boundary layer thickness rises with uplifting values of the unsteady parameter. Sarojamma et al [46] made a numerical investigation on the characteristics of micropolar fluid flow with the Cattaneo–Christov heat flux model. The study concluded that the concentration of chemical reaction rises with a growing diffusion ratio parameter. Shamshuddin and Satya Narayana [59] studied the effects of non-Fourier heat flux on the dynamics of squeezing flow past a Riga plate. They solved the system of equations by shooting method and concluded that the local heat transfer coefficient upsurges with increasing Eckert number. On thesamegrounds, manyauthors (Alshomrani et al[5], Sultan et al[63], Hayat et al [27], Horuz et al [28], Waqas et al [71]) numerically studied the influence of AE on different fluid flow models. Faisal et al [38] explored the dynamical aspects of thermodiffusion and diffusothermal effects over a stretched surface with variable viscosity. They solved the coupled ordinary differential equation (ODE) system by using the shooting technique and concluded that the nondimensional velocity of fluid rises with a growing temperature dependent viscosity parameter. Gogula Sandhya [20] have described the Buoyancy forces and activation energy on the MHD radiative flow over an exponentially stretching sheet with second-order slip. Several authors have been evaluated to effect of Arrhenius activation energy and dual stratifications on the MHD flow of a Maxwell nanofluid with various heating (Sandhya et al. [20], Zeeshan et al. [73], Saida Rashid et al. [55], Gireesha et al. [19]). Khan et al [36], Ijaj Khan [30], made brief discussion on Activation Energy impact in Nonlinear Radiative Stagnation Point Flow of Cross Nanofluid and also analysed the Arrchenius activation energy impact in binary chemically reactive flow of TiO_2-Cu-H2O hybird nanomaterial, Shafiq Ahmad and Sohail Nadeem [57] have discussed to analysis of activation energy and its impact of hybrid nanofluid in the presence of Hall and ion slip currents.

In this paper, we investigate effect of variable viscosity, activation energy on natural convective heat and mass transfer flow over a vertical wavy surface embedded in a fluid saturated porous medium in the presence of heart generating source. The vertical wavy wall and the governing equations for flow heat and mass transfer are transformed to a plane geometry case by employing the Rungre-Kutta fourth order with Shooting technique. The non-dimensional velocity, temperature and nano-concentration graphs as well as skin friction ,rate of heat and mass transfer coefficients are displayed for different values of thermal

radiation, heat source, chemical reaction parameter and amplitude of the wavy surface. The obtained results are compared with those presented by Bejan and Khair[9] and Lai[41] and excellent agreement has been reported in the absence of thermal radiation, heat source and variable properties.

2.Formulation Of The Problem:

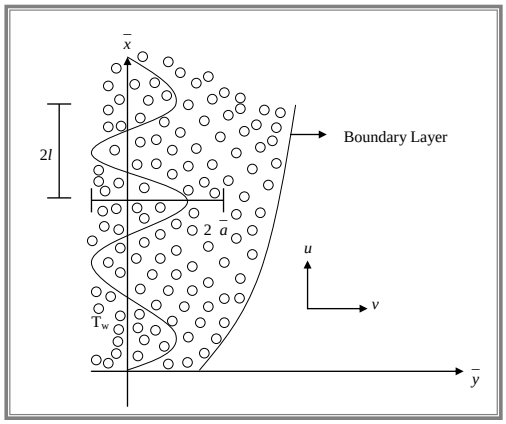

Fig. – 1 : Physical Configuration and Co-ordinate System

We consider a steady incompressible two-dimensional laminar natural convective heat and mass transfer flow of a nanofluid over a vertical wavy surface embedded in a saturated porous medium. The porous medium is uniform and local thermal equilibrium with the fluid. The Darcy law is used to describe the fluid saturated porous medium. The fluid is assumed to be gray absorbing-emitting radiation but non-scattering medium. The wavy surface profile is given by

$$y = \bar{\sigma}(\bar{x}) = \bar{a}Sin(\frac{\pi \bar{x}}{l})$$

where l is the characteristic length of wavy surface and $\bar{a}$ is the amplitude of the wavy surface. The wavy surface is maintained at constant temperature Tw which are higher than the ambient fluid temperature T_∞.

We consider the natural convection-radiation flow in the presence of heat sources to be governed by the following equations under Boussinesq approximations:

$$\frac{\partial u}{\partial x} + \frac{\partial v}{\partial y} = 0 \qquad (2.1)$$

$$(\frac{\mu_f(T)}{k})u = -\frac{\partial p}{\partial x} + g(1-C_\infty)\beta\rho_{f_\infty}\beta g(T-T_\infty) - (\rho_p - \rho_{f_\infty})kg(C-C_\infty) - (\sigma_{nf}\mu_e^2 H_0^2)u + (\frac{Cb}{k})u^2 \qquad (2.2)$$

$$(\frac{\mu_f(T)}{k})v = -\frac{\partial p}{\partial y} + (\frac{Cb}{k})v^2 \qquad (2.3)$$

$$u\frac{\partial T}{\partial x}+v\frac{\partial T}{\partial y}=\frac{k_f}{\rho_f C_p}\frac{\partial^2 T}{\partial y^2}+\tau\{D_B(\frac{\partial T}{\partial x}\frac{\partial C}{\partial x}+\frac{\partial T}{\partial y}\frac{\partial C}{\partial y})+\frac{D_T}{T_\infty}((\frac{\partial T}{\partial y})^2+(\frac{\partial T}{\partial y})^2)]- \\ -(\frac{1}{\rho C_p})\frac{\partial(q_R)}{\partial y}+\frac{q'''}{\rho C_p}+2\mu_f(T)(u_y^2+v_y^2) \quad (2.4)$$

$$u\frac{\partial C}{\partial x}+v\frac{\partial C}{\partial y}=D_B(\frac{\partial^2 C}{\partial x^2}+\frac{\partial^2 C}{\partial y^2})+\frac{D_T}{T_\infty}(\frac{\partial^2 T}{\partial x^2}+\frac{\partial^2 T}{\partial y^2})-kc(\frac{T}{T_\infty})^n Exp(-\frac{E_n}{KT})(C-C_\infty) \quad (2.5)$$

The relevant boundary conditions are

$$\vec{u}=0,\vec{v}=0,T=T_w\ ,C=C_w\ \ at\ \ \bar{y}=\bar{\sigma}(\bar{x})=\bar{a}\ Sin(\frac{\pi\bar{x}}{l})$$

$$\vec{u}=0,T\to T_\infty\ ,C\to C_\infty\ \ as\ \ \ \bar{y}\to\infty \quad (2.6)$$

Where $\bar{u}$ and $\bar{v}$ are the volume averaged velocity components in the directions of x and y respectively T,C are temperature, Concentration respectively, ρ is the density of the fluid, μ is the dynamic viscosity of the fluid , k is the permeability of the porous medium , σ is the electrical conductivity, μ_e is the magnetic permeability, Ho is the strength of the magnetic field , D_B is the Brownian diffusion coefficient and D_T is the thermophoretic diffusion coefficient, $\tau=\frac{(\rho C_p)}{(\rho C_f)}$ is the ratio between the effective heat capacity of the nanoparticle material and heat capacity of the fluid,, kc is the coefficient of chemical reaction, β_o are the coefficients of thermal expansion, α is the thermal conductivity , q_r is the radiative heat flux ,g is the acceleration due to gravity , q''' is rate of internal heat generation (>0) or absorption(<0) coefficient and Q_H is the strength of the heat source.

The nanofluid dynamic viscosity is assumed to be the exponential decreasing function of temperature given by

$$\mu_f=\mu_\infty\exp(-\beta(T-T_\infty)) \quad (2.7)$$

Where μ_∞ is the free stream dynamic viscosity at temperature

The internal heat generation or absorption term q''' is mideled according to the following equation

$$q'''=\frac{kRa}{L^2\xi}[A^\bullet(T_w-T_\infty)f'+B^\bullet(T-T_\infty)]$$

Where $A^\bullet$ and $B^\bullet$ are the coefficient of space and temperature dependent heat source/sink respectively. It is to be noted that the case $A^\bullet>0, B^\bullet>0$ corresponds to internal heat generation while $A^\bullet<0, B^\bullet<0$,corresponds to internal heat absorption.

By applying Rosseland approximation (Brewester [10]) the radiative heat flux q_r is given by

$$q_r=-\left(\frac{4\sigma^*}{3\beta_R}\right)\frac{\partial}{\partial y}\left[T'^4\right] \quad (2.8)$$

Where σ* is the Stephan – Boltzmann constant and mean absorption coefficient.

Assuming that the difference in temperature within the flow are such that T'^4 can be expressed as a linear combination of the temperature. We expand T'^4 in Taylor's series about Te as follows

$$T'^4 = T_\infty^4 + 4T_0^3(T - T_0) + 6T_0^2(T - T_0) + \ldots\ldots \tag{2.9}$$

Neglecting higher order terms beyond the first degree in $(T - T_\infty)$ .we have

$$T'^4 \cong -3T_0^4 + 4T_0^3 T \tag{2.10}$$

Differentiating equation (2.8) with respect to y and using (2.10) we get

$$\frac{\partial(q_R)}{\partial y} = -\frac{16\sigma^* T_0^3}{3\beta_R}\frac{\partial^2 T}{\partial y^2} \tag{2.11}$$

On using equations (2.11) in the last term of equation (2.4) we get

$$\frac{1}{k}(\mu_f e^{-m(T-T_\infty)}(\frac{\partial u}{\partial y} - \frac{\partial v}{\partial x}) + \mu_f m e^{-m(T-T_\infty)}(u\frac{\partial T}{\partial y} - v\frac{\partial T}{\partial x}) - \sigma_{nf}\mu_e H_o^2(\frac{\partial^2 u}{\partial y^2}) - \frac{2C_b}{\sqrt{k}}(u\frac{\partial u}{\partial y}) \tag{2.12}$$

$$\left.\begin{aligned}\rho C_p(\bar{u}\frac{\partial T}{\partial \bar{x}} + \bar{v}\frac{\partial T}{\partial \bar{y}}) = k_f(\frac{\partial^2 T}{\partial x^2} + \frac{\partial^2 T}{\partial y^2}) + \frac{16\sigma^\bullet T_\infty^3}{3\beta_R}(\frac{\partial^2 T}{\partial x^2} + \frac{\partial^2 T}{\partial y^2}) + \\ + \frac{kRa}{L^2\xi}[A^\bullet(T_w - T_\infty)f' + B^\bullet(T - T_\infty)]/\rho C_p + 2\mu_f(T)(\frac{\partial u}{\partial y})^2 + (\frac{\partial v}{\partial x})^2)\end{aligned}\right| \tag{2.13}$$

$$u\frac{\partial C}{\partial x} + v\frac{\partial C}{\partial y} = D_B(\frac{\partial^2 C}{\partial x^2} + \frac{\partial^2 C}{\partial y^2}) + \frac{D_T}{T_\infty}(\frac{\partial^2 T}{\partial x^2} + \frac{\partial^2 T}{\partial y^2}) - kc(\frac{T}{T_\infty})^n Exp(-\frac{E_n}{KT})(C - C_\infty) \tag{2.14}$$

In view of the continuity equation(2.1) we define the stream function ψ as

$$\bar{u} = \frac{\partial \bar{\psi}}{\partial \bar{y}} \quad , v = -\frac{\partial \bar{\psi}}{\partial \bar{x}} \tag{2.15}$$

In order to write the governing equations in the dimensionless form we introduce the following non-dimensional variables as

$$x = \frac{\bar{x}}{l}, y = \frac{\bar{y}}{l}, a = \frac{\bar{a}}{l}, \sigma = \frac{\bar{\sigma}}{l}, \psi^* = \frac{\bar{\psi}}{l}, \theta = \frac{T - T_\infty}{T_w - T_\infty}, \phi = \frac{C - C_\infty}{C_w - C_\infty} \tag{2.16}$$

Using the equations (2.15)-(2.16).equations(2.12).(2.14) reduce to

$$\left.\begin{aligned}e^{-B\theta}(\frac{\partial^2 \psi^\bullet}{\partial x^2} + \frac{\partial^2 \psi^\bullet}{\partial y^2}) - M^2\frac{\partial^2 \psi^\bullet}{\partial y^2} - Be^{-B\theta}(\frac{\partial \theta}{\partial y}\frac{\partial \psi}{\partial y} + \frac{\partial \theta}{\partial x}\frac{\partial \psi}{\partial x}) = Ra(\frac{\partial \theta}{\partial y} - Nr\frac{\partial \phi}{\partial y}) - \\ - fs(\frac{\partial \psi^\bullet}{\partial y}\frac{\partial^2 \psi^\bullet}{\partial y^2} - \frac{\partial \psi^\bullet}{\partial x}\frac{\partial^2 \psi^\bullet}{\partial x^2})\end{aligned}\right| \tag{2.17}$$

$$\left.\begin{aligned}(1 + \frac{4Rd}{3})(\frac{\partial^2 \theta}{\partial \bar{x}^2} + \frac{\partial^2 \theta}{\partial \bar{y}^2}) + Nb(\frac{\partial \theta}{\partial \bar{x}}\frac{\partial \phi^\bullet}{\partial \bar{y}} + \frac{\partial \theta}{\partial \bar{y}}\frac{\partial \phi^\bullet}{\partial \bar{x}}) + Nt((\frac{\partial \theta}{\partial \bar{x}})^2 + (\frac{\partial \theta}{\partial y})^2) + \\ + A1f' + B1\theta = (\frac{\partial \theta}{\partial x}\frac{\partial \psi^\bullet}{\partial y} - \frac{\partial \theta}{\partial y}\frac{\partial \psi^\bullet}{\partial x}) + 2e^{-B\theta}((\frac{\partial^2 \psi^\bullet}{\partial x^2})^2 + (\frac{\partial^2 \psi^\bullet}{\partial y^2})^2)\end{aligned}\right| \tag{2.18}$$

$$\left.\begin{aligned}\frac{1}{Le}(\frac{\partial^2 \phi}{\partial \bar{x}^2} + \frac{\partial^2 \phi}{\partial \bar{y}^2}) + (\frac{Nt}{Nb})(\frac{\partial^2 \phi}{\partial \bar{x}^2} + \frac{\partial^2 \phi}{\partial \bar{y}^2}) - \\ - Le\gamma(1 + n\delta\theta)\exp(-\frac{E_1}{(1 + \delta\theta)})\phi = -(\frac{\partial \phi}{\partial \bar{x}}\frac{\partial \psi^\bullet}{\partial \bar{y}} - \frac{\partial \phi}{\partial \bar{y}}\frac{\partial \psi^\bullet}{\partial \bar{x}})\end{aligned}\right| \tag{2.19}$$

Where $Ra = \frac{Lg\beta(T_w - T_\infty)(1-C_\infty)}{a\mu}$ is the Darcy-Rayleigh number, $\nu = \frac{\mu_\infty}{\rho}$ is the kinematic viscosity of the fluid, $Rd = \frac{4\sigma^* T_\infty^3}{k_f \beta_R}$ is the Radiation parameter, $M^2 = \frac{\sigma \mu_e^2 H_0^2 l^2}{\mu}$ .is the magnetic parameter. , $Le = \frac{\nu}{D_B}$ is the Lewis number, $\gamma = \frac{kcL^2}{D_B}$ is the chemical reaction parameter , $N_r = \frac{(\rho_p - \rho_{f\infty})(C_w - C_\infty)}{\rho_{f\infty}(1-C_\infty)(T_w - T_\infty)}$ is the buoyancy ratio , $N_b = \frac{\tau D_B (C_w - C_\infty)}{a}$ is Brownian motion parameter, $N_t = \frac{\tau D_T (T_w - T_\infty)}{aT_\infty}$ is Thermophoresis parameter.

$\theta_w = \frac{T_w}{T_\infty}, \delta = \theta_w - 1$ is the temperature difference parameter, $E1 = \frac{E_n}{k_f T_\infty}$ is the activation energy parameter. $B = m(T_w - T_\infty),, Ec = \frac{(u_w)^2}{C_p(T_w - T_\infty)}$

The transformed boundary conditions are

$$\psi^\bullet = 0, \theta = 1, \phi = 1 \ \ at \ \ y = aSin(x)$$
$$\frac{\partial \psi^\bullet}{\partial y} \to 0, \theta \to 0, \phi \to \infty \ as \ y \to \infty \qquad (2.20)$$

We can transform the effect of wavy surface from the boundary conditions into the governing equations by using suitable coordinate transformation with boundary layer scaling for the case of free convection .The Cartesian coordinates(xy) are transformed into the new variables($\xi \ \eta$).

We incorporate the effect of effect of wavy surface and the usual boundary layer scaling into the governing equations(2.17)-(2.19) for free convection using the transformations and $Ra \to \infty$(i.e boundary layer approximation)

$$x = \xi, \bar{\eta} = \frac{y - aSin(x)}{\xi^{1/2} Ra^{-1/2}}, \psi^* = Ra^{1/2}\psi$$

These transformations are similar to those presented in for instance. We obtain the following boundary layer equations :

$$\left.\begin{aligned} &\mathbf{B}e^{-B\theta}(1 + a^2Cos^2\xi)\frac{\partial\theta}{\partial\eta}\frac{\partial\psi}{\partial\eta} + (1 + a^2Cos^2\xi)e^{-B\theta}\frac{\partial^2\psi}{\partial\eta^2} = Ra\,\xi^{1/2}(\frac{\partial\theta}{\partial\eta} - Nr\frac{\partial\phi}{\partial\eta}) - \\ &- M^2\frac{\partial^2\psi}{\partial\eta^2} - fs(1 + a^3Cos^3(\xi))\frac{\partial\psi^\bullet}{\partial\eta}\frac{\partial^2\psi^\bullet}{\partial\eta^2} \end{aligned}\right| \qquad (2.21)$$

$$\left.\begin{aligned} &\xi^{1/2}(\frac{\partial\theta}{\partial\xi}\frac{\partial\psi}{\partial\eta} - \frac{\partial\theta}{\partial\eta}\frac{\partial\psi}{\partial\xi}) = (1 + a^2Cos^2(\xi))((1 + \frac{4Rd}{3})(\frac{\partial^2\theta}{\partial\eta^2}) + \\ &+ Nb\frac{\partial\theta}{\partial\eta}\frac{\partial\phi}{\partial\eta} + Nt(\frac{\partial\theta}{\partial\eta})^2 + A1f' + B1\theta + 2e^{-B\theta}Ec(\frac{(1 + a^4Cos^4(\xi)}{(1 + a^2Cos^2(\xi)^2}(\frac{\partial^2\psi}{\partial\eta^2})^2 \end{aligned}\right| \qquad (2.22)$$

$$\xi^{1/2} Le\left(\frac{\partial\phi}{\partial\xi}\frac{\partial\psi}{\partial\eta}-\frac{\partial\phi}{\partial\eta}\frac{\partial\psi}{\partial\xi}\right)=(1+a^2Cos^2(\xi))\left(\frac{\partial^2\phi}{\partial\eta^2}+\frac{Nt}{Nb}\frac{\partial^2\phi}{\partial\eta^2}\right)- \left| -Le\gamma(1+n\delta\theta)\exp\left(-\frac{E_1}{(1+\delta\theta)}\right)\phi \right. \quad (2.23)$$

3. Soulution Methodology:

We now introduce the following similarity variables as

$$\eta=\frac{\bar{\eta}}{(1+a^2Cos^2(\xi))},\psi=\xi^{1/2}f(\eta),\theta=\theta(\eta),,\phi=\phi(\eta)$$

In equations(2.20)-(2.22)we obtain a system of ordinary differential equations as follows:

$$(f''+\mathbf{B}\theta' f')Exp(-B\theta)-\frac{M^2}{(1+a^2Cos^2\xi)}f''-Ra(\theta'-Nr\,\phi')-fs\frac{(1+a^3Cos^3(\xi))}{(1+a^2Cos2(\xi))^3}f'f'' \quad (2.24)$$

$$\left(1+\frac{4Rd}{3}\right)\theta''+\frac{1}{2}f\theta'+Nb\,\theta'\phi'+Nt(\theta')^2+\frac{A^{\bullet}f'+B^{\bullet}\theta}{(1+a^2Cos^2(\xi))}+ \left| +2e^{-B\theta}Ec\left(\frac{(1+a^4Cos^4(\xi)}{(1+a^2Cos^2(\xi)^3}(f'')^2\right. \quad (2.25)$$

$$\phi''+\frac{Le}{2}f\phi'+\left(\frac{Nt}{Nb}\right)\theta''-Le\gamma(1+n\delta\theta)\exp\left(-\frac{E_1}{(1+\delta\theta)}\right)\phi=0 \quad (2.26)$$

Where prime denotes differentiation with respect to η.

The corresponding boundary conditions are

$f=0$ θ=1 $\phi=1$ at $\eta=0$ (2.27)

$f'\to 0$ θ→0 $\phi\to 0$ as $\eta\to\infty$

In equation(2.25) the radiation parameter $Rd=\frac{4\sigma^* T_\infty^3}{k_f\beta_R}$ means that the rate of thermal radiation contribution relative to the thermal conditions. As $Rd\to\infty$influence of thermal radiation is high in the boundary layer regime. For $Rd\to 0$the term 4Rd/3 tends to zero. For Rd=1thermal radiation and thermal conduction will give equal contribution.

The main results of practical interest in many applications are heat transfer coefficient mass transfer coefficient at the surface. The drag,heat and mass transfer coefficients are expressed in terms of skin friction, Nusselt and Sherwood numbers C_f, Nux, Shx.

Skin friction, (C_f),Nusselt number(Nux) and Sherwood number(Shx) are defined in terms of Ra_x and the amplitude 'a' as

$$Nux=\frac{xq_w}{\alpha_o(T_w-T_\infty)},\quad Shx=\frac{xm_w}{D_b(C_w-C_\infty)} \quad (2.28)$$

Where q_w is the heat flux on the wavy surface and is defined by

$q_w=-\alpha_0\bar{n}.\nabla T$ *and* $\bar{n}=\left(-\frac{aCos(\xi)}{\sqrt{(1+a^2Cos^2(\xi))}},\frac{1}{\sqrt{(1+a^2Cos^2(\xi))}}\right)$ is the unit normal vector to the wavy surface α_0 is the effective porous medium thermal conductivity. Therefore

$$C_f = \frac{f''(0)(1+a^2Cos^2(\xi))Ra_x^{1/2}}{(1+M^2+a^2Cos^2(\xi))}, Nu_\xi = -\frac{\theta'(0)Ra_\xi^{1/2}}{\sqrt{(1+a^2Cos^2(\xi))}},$$

$$Sh_\xi = -\frac{\phi'(0)Ra_x^{1/2}}{(1+a^2Cos^2(\xi))} \quad (2.29)$$

4. Conversion

In the absence of magnetic field(M=0) and heat sources(Q=0), chemical reaction(γ=0) the results are in good agreement with Vendabai et al [70]. In absence of variable viscosity(B=0) and activation energy (E1=0,δ=0),Dissipation(Ec=0) the results are in good agreement with Srinivasa Reddy[64].

Table – 2 : Nusselt Number (Nu) and Sherwood Number (Sh) at η = 0

Srinivasa Reddy [64]					Present Results		
Parameter		**Cfx (0)**	**Nu(0)**	**Sh(0)**	**Cfx (0)**	**Nu(0)**	**Sh(0)**
Nr	0.5	-0.384728	0.632326	0.483994	-0.384622	0.632251	0.483878
	1.5	-0.282569	0.401604	0.642376	-0.282490	0.401586	0.642176
	3.5	-0.114149	0.283594	0.706004	-0.114098	0.283447	0.706118
	5.0	-0.089765	0.201113	0.765433	-0.089644	0.201096	0.765523
Q	-0.2	-0.384728	0.63236	0.483994	-0.384614	0.63228	0.483824
	-0.4	-0.624463	0.80624	0.334334	-0.624329	0.80575	0.334232
	0.2	0.340236	0.111467	0.869649	0.340206	0.111387	0.869550
	0.4	0.0202877	0.394523	0.835568	0.0202759	0.394499	0.835473
Nb	0.1	-0.553868	0.644392	0.157567	-0.553829	0.644266	0.157459
	0.3	-0.384728	0.632362	0.483994	-0.384706	0.632286	0.483894
	0.4	-0.305298	0.607824	0.597559	-0.305209	0.607728	0.597543
	0.5	-0.250486	0.580872	0.655284	-0.250409	0.580789	0.655276
Nt	0.1	-0.349288	0.661968	0.617011	-0.349225	0.661862	0.616903
	0.2	-0.384728	0.632362	0.483994	-0.384655	0.632183	0.483846
	0.3	-0.414809	0.606086	0.368148	-0.414755	0.606068	0.368044
	0.4	-0.440432	0.582556	0.266607	-0.440359	0.582447	0.266599
γ	0.5	-0.384728	0.632363	0.483994	-0.384655	0.632186	0.483846
	1.5	-0.090005	0.636184	1.090582	-0.089955	0.636092	1.090492
	-0.5	0.272864	0.218057	0.766389	0.272755	0.218027	0.766279
	-1.5	3.134835	0.461636	6.895882	3.134805	0.461526	6.895724
a	0.1	-0.384728	0.632362	0.483994	-0.384629	0.632228	0.483812
	0.2	-0.384686	0.628091	0.480429	-0.384644	0.628041	0.480328
	0.3	-0.384157	0.621734	0.475222	-0.384105	0.621689	0.475188
	0.4	-0.380188	0.602947	0.460132	-0.380165	0.602879	0.460031
ξ	π/6	-0.384742	0.631729	0.483464	-0.384695	0.631649	0.483246
	π/4	-0.384728	0.632362	0.483994	-0.384708	0.632186	0.483846
	π/3	-0.384705	0.632992	0.484527	-0.384625	0.632822	0.484426

Srinivasa Reddy [64]				
Parameter		Cfx (0)	Nu(0)	Sh(0)
	$\pi/2$	-0.384676	0.633624	0.485062

Present Results		
Cfx (0)	Nu(0)	Sh(0)
-0.384605	0.633524	0.484826

5. Results And Discussion:

Figs.2a-2d illustrate the variation of velocity temperature and nano-concentration with Rayleigh number(Ra). It can observed from the profiles that the axial and secondary velocities enhances in the flow region. An increase in Ra reduces the temperature and in the case of the nano-concentration, Ra reduces it in the region(0,1.5),enhances in the region (1.5,5) .This may be attributed to the fact that the thickness of the momentum boundary layer grows with increasing values of Ra. Also the thickness of the thermal boundary layer decays with increasing Ra. Solutal layer reduces in a narrow region adjacent to the wall and grows far away from the wall. From the profiles we find that the velocities reduces in the region with increasing M .The temperature upsurges in (0,5) and the nano-concentration decays in the region(0,1.5),enhances far away from the wall with increasing values of magnetic parameter.

Figs.3 represent the effect of porous parameter(K)on the flow variables. From the profiles we find that the velocities depreciate in the flow region(0,5) with increasing values of porous parameter(K).The temperature increases in (0,5) and the nano-concentration decays in the region(0,1.5),enhances far away from the wall with increasing values of magnetic parameter. Thus higher the porous permeability smaller the thickness of the momentum and larger the thermal boundary layer .With respect to buoyancy parameter(N)(fig.3b) we find that when the molecular buoyancy force dominates over the thermal buoyancy force the primary velocity increases and secondary velocity reduces when the buoyancy forces are in the same direction. The temperature enhances with increase in N. Also the nano-concentration reduces in the region(0,1.5) and enhances in the region(1.5,4.0) with increasing N(Fig.3d) .

Figs.4a-4d represent u,v ,θ and ϕ with temperature dependent heat source parameter(Q).From the profiles we note that the primary velocity (u) reduces with Q>0 in the region(0,0.75) and in the region(0.75,1.5)it increases with Q. For Q<0,the primary velocity grows in the region (0.5).In both the velocities, temperature upsurge in the presence of heat generating sources while in the case of heat absorbing source, they depreciate in the flow region. This may be attributed to the fact that in the presence of heat generating sources, heat is generated and heat is absorbed in the case of heat absorbing sources which leads to the thickening of the momentum and thermal boundary layer. The concentration reduces with Q>0 and grows with Q<0 in the flow region ,this indicates that the thickness of the solutal boundary layer becomes thicker with Q>0 and thinner with higher values of Q<0(figs. 4a-4d).

Figs.5a-5d show the variation of velocity, temperature and nano-concentration with the influence of radiation parameter(Rd) and viscosity parameter(B).From fig.5a we find that both velocities reduce in the region(0,4) .This means that the thickness of the momentum boundary layer reduces with increasing values of Rd. Fig.5b &5c represent the temperature and nano-concentration with Rd. It can be seen from the profiles that an increase in Rd leads to thickening of the thermal boundary layer reduces. The solutal boundary layer becomes

thinner in the region(0,1.5) and thicker in far away from the wall with increasing Rd which results in an enhancement of the temperature and depreciation in the nano-concentration in the flow region. Higher the viscosity parameter(B) larger the velocities smaller the temperature. The nano-concentration decays the thickness of the solutal layer in the narrow region(0,1.5) and grows in the region far away from the wall(fig.5d)

The impact of Nb, Nt on u,v,θ and ϕ can be seen from figs.6a-6d.An increase in Brownian motion parameter(Nb) reduces the primary velocity in the flow region(0,1.5) and enhances in the flow region(1.5,4.0) while increase in thermophoresis parameter(Nt) upsurges in (0,1.5) and depreciates in the region(1.5,4.0).The secondary velocity(g) and nano-concentration (ϕ)reduces with Nb and enhances with Nt in the flow region(0,4.0).The temperature (θ) experiences with rising values of Nb and Nt ion the flow region(0,4.0).Thus the thermal boundary layer becomes thicker with increasing Nb and Nt.

Figs.7a-7c represent the velocity, temperature and nano-concentration with chemical reaction parameter(γ).It can be seen from the profiles that the primary velocity reduces in the flow region (0,1) and enhances in the remaining flow region in the degenerating chemical reaction case while in the generating case it depreciates in the entire flow region.(fig.5a).The secondary velocity, temperature and nano-concentration reduces ion the degenerating chemical reaction case and upsurge in the generating case(figs.7b-7d).

The effect of activation energy(E1) and temperature difference parameter(δ) on u,v,θ and ϕ can be seen from figs.8a-8d.An increase in temperature difference(δ) reduces primary velocity ,temperature and nano-concentration in the flow region. The secondary velocity(v) upsurges with increasing values of δ.The primary velocity(u) increases in a narrow region(0,1.0) and decreases in (1.0,4.0) with increasing values of activation energy parameter(E1)The secondary velocity reduces and temperature elevates with rising values of E1 in the flow region(0,4.0). The activation energy(E1) concentrate more as a result of function of Arrhenius. Increasing values of E1 reduces the concentration monotonically close to the surface and far away from the wall while a significant augmentation persists in the central region. Generally, Activation energy is the minimum amount of energy that is required for a chemical reaction to stimulate atoms or molecules in the reaction. There should be a considerable number of atoms whose Activation energy is less than or equal to translational energy in a chemical reaction. In many engineering applications, activation energy may be considered as a better coolant.

Figs.9a-9d depict the variation of u,v θ and ϕ with stream wise coordinate (ξ).and amplitude(a). We find that an increase in amplitude(a) / stream wise coordinate (ξ) decreases the velocities, and increases the temperature in the flow region. The nano-concentration (ϕ) reduces in the flow region(0,1.5) and upsurges in the region(1.5,4.0) with rising values of ‘a’ and ‘ξ’ .

An increased in Lewis number (Le)/index number(n) enhances the primary velocity(u),reduces the secondary velocity, temperature and nano-concentration in the flow region(figs.10a-10c)

The skin friction(Cfx&Cfz)at the wall is represented in table.2 for different parametric variations. From the tabular values we find that the magnitude of the skin friction Cfx reduces and Cfz enhances with increase in Ra .Higher the Lorentz force/lesser the

permeability smaller the stress components at $\eta = 0$.When the molecular buoyancy force dominates over the thermal buoyancy force Cfx enhances and Cfz reduces at the wall when the buoyancy forces are in the same direction. Higher the thermal radiation(Rd) larger Cfx and smaller Cfz at the wall. For higher values of variable viscosity(B)/Brownian motion parameter(Nb)/ thermophoresis parameter(Nt) larger the stress components at the wall. In the presence heat generating heat source(Q>0), Cfx enhances and Cfz reduces at the wall while they experience an enhancement at the wall in the presence of heat absorbing source. Cfx grows and Cfz decays at the wall in the degenerating chemical reaction case while in the generating case,both stress components decays at the wall. Cfx and Cfz reduces with activation energy parameter(E1) and grow with temperature difference parameter(δ) at the wall. Cfx and Cfz decays with higher values of amplitude (a) of the wavy wall. Also Cfx upsurges and Cfz decays with rising values of stream wise coordinate(ξ)|/Lewis number(Le).Higher the index number(n) larger the stress components at the wall. The rate of heat transfer(Nu) and mass transfer at the wall is displayed in table.2. From the tabular values we find that rate of heat and mass transfer at the wall increase with increase in Rayleigh number(Ra)and reduces with increasing magnetic parameter(M)/porous parameter(K)/buoyancy ratio(N).An increase in Q>0 reduces Nu and enhances Sh at the wall while a reversed effect is noticed at the wall in the presence of heat absorbing source(Q<0).Nu and Sh decays with raising values of radiation parameter(Rd)and grows with viscosity parameter(B).An increase in Nb reduces Nu and Sh at the wall while Nu reduces with Nb ,grows with Nt at the wall.The Nusselt number Nu grows and Sh decays at the wall in the degenerating chemical reaction case while in the generating case, Nh and Sh decay at the wall. Higher the activation energy parameter(E1) /amplitude(a),smaller Nu and Sh at the wall. An increase in temperature difference parameter(δ)/Lewis number(Le)/index number(n),leads to an increment in Nu and Sh at the wall. Higher the stream wise coordinate(ξ) smaller Nu and larger Sh at the wall.

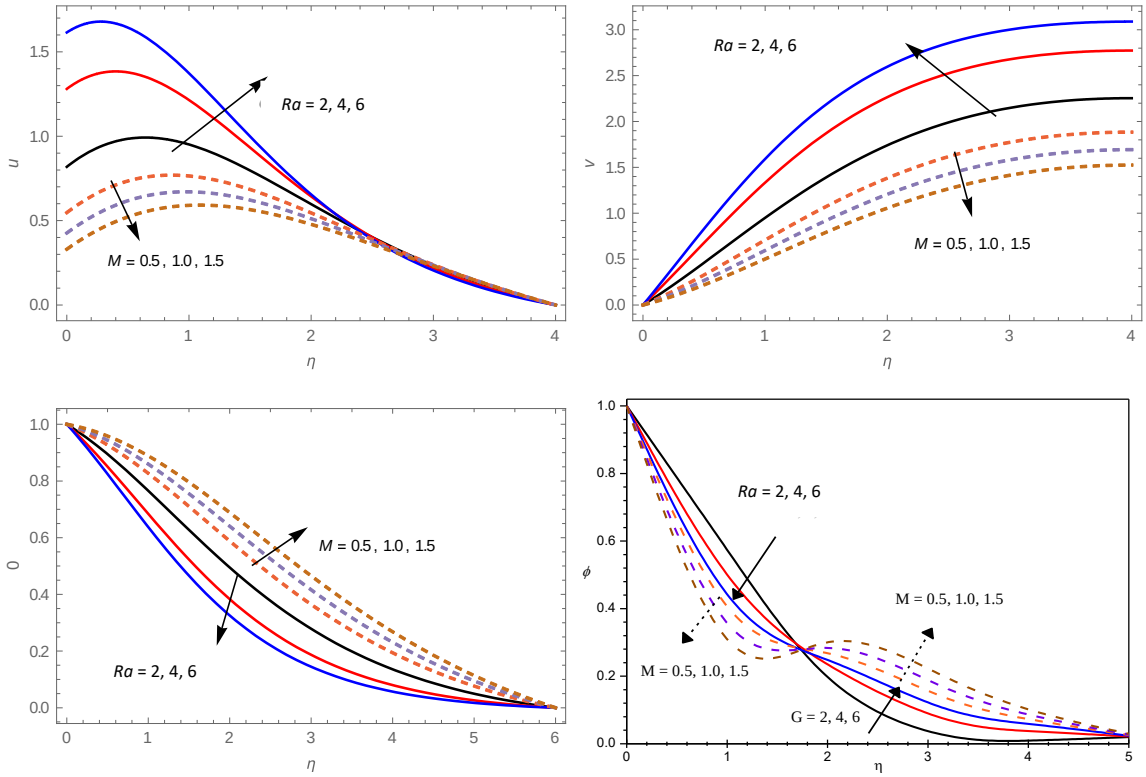

Fig.2: Variation of [a].axial velocity(u), [b].Secondary Velocity(v), [c].Temperature(θ), [d].Nanoconcentration(ϕ) with Ra and M

K=0.2,N=0.5,Rd=0.5,Q=0.5, γ=0.2,Nb=0.1,Nt=0.1,E1=0.1,δ=0.1,a=0.1,ξ=π/4,Le=1,n=1

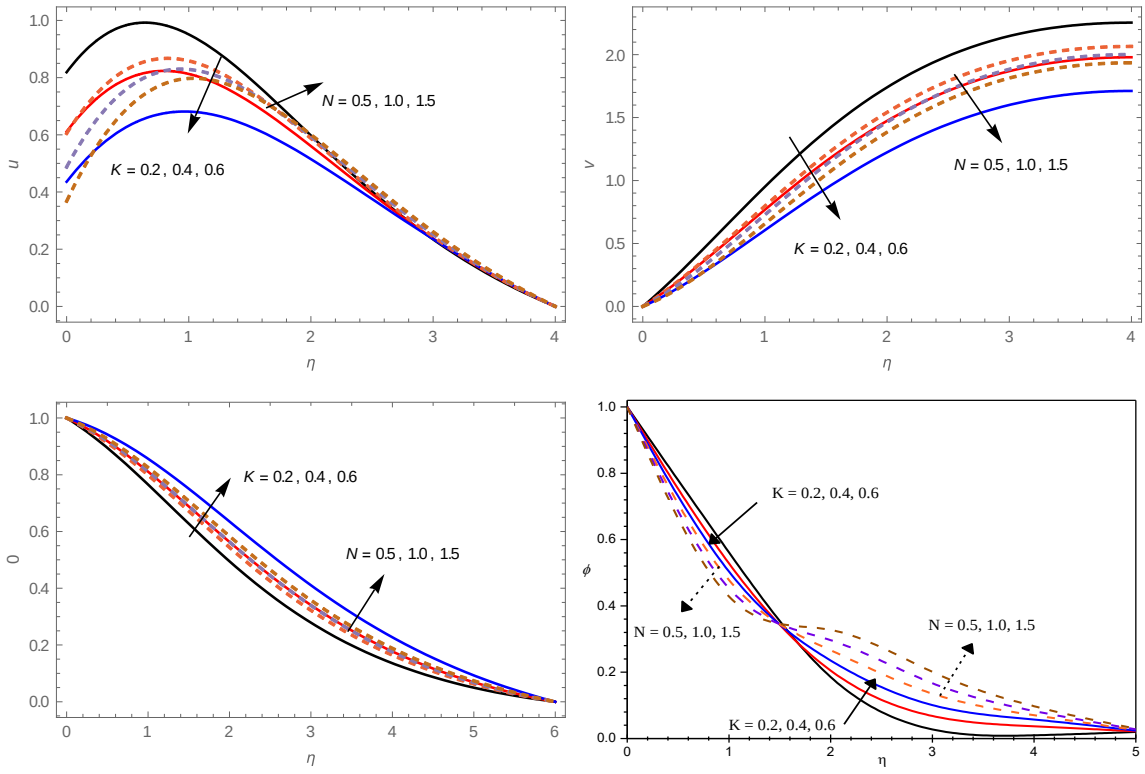

Fig.3: Variation of [a].axial velocity(u), [b].Secondary Velocity(v), [c].Temperature(θ), [d].Nanoconcentration(ϕ) with K and N

Ra=2,M=0.5,Rd=0.5,B=0.2,Q=0.5,
γ=0.2,Nb=0.1,Nt=0.1,E1=0.1,δ=0.1,a=0.1,ξ=π/4,Le=1,n=1

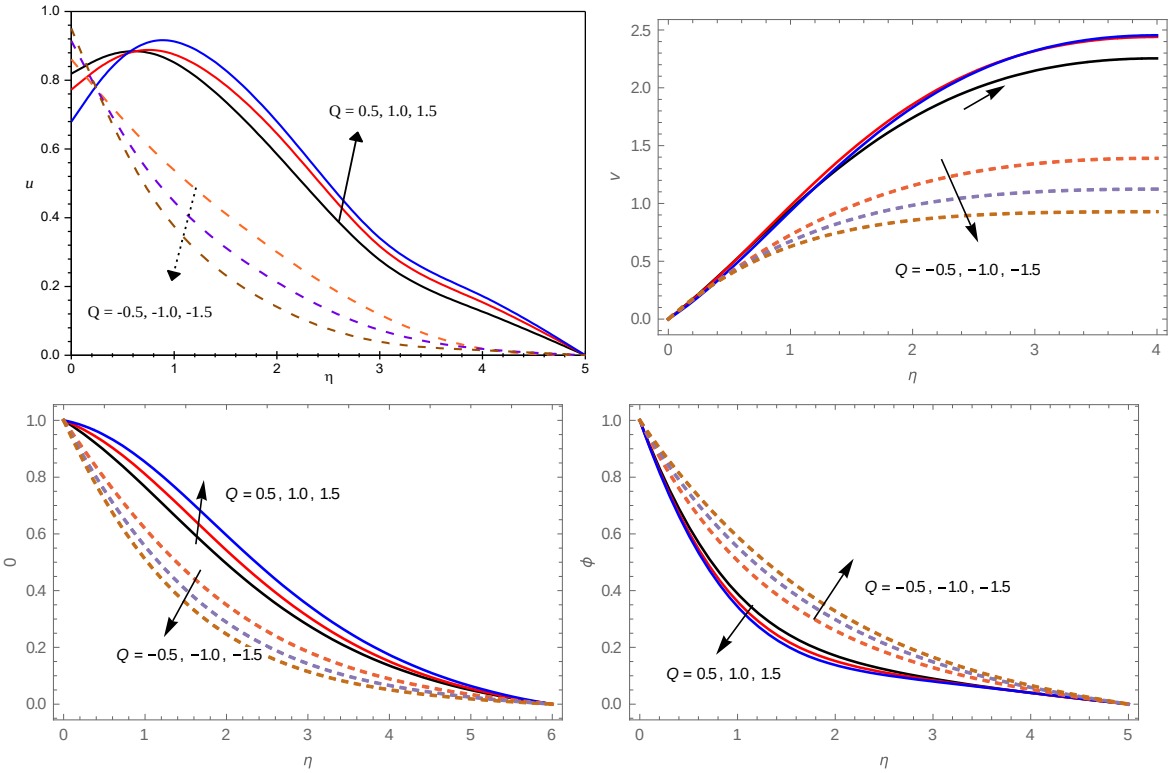

Fig.4: Variation of [a].axial velocity(u), [b].Secondary Velocity(v), [c].Temperature(θ), [d].Nanoconcentration(ϕ) with Q

Ra=2,M=0.5,K=0.2,N=0.5,Rd=0.5,B=0.2,
γ=0.2,Nb=0.1,Nt=0.1,E1=0.1,δ=0.1,a=0.1,ξ=π/4,Le=1,n=1

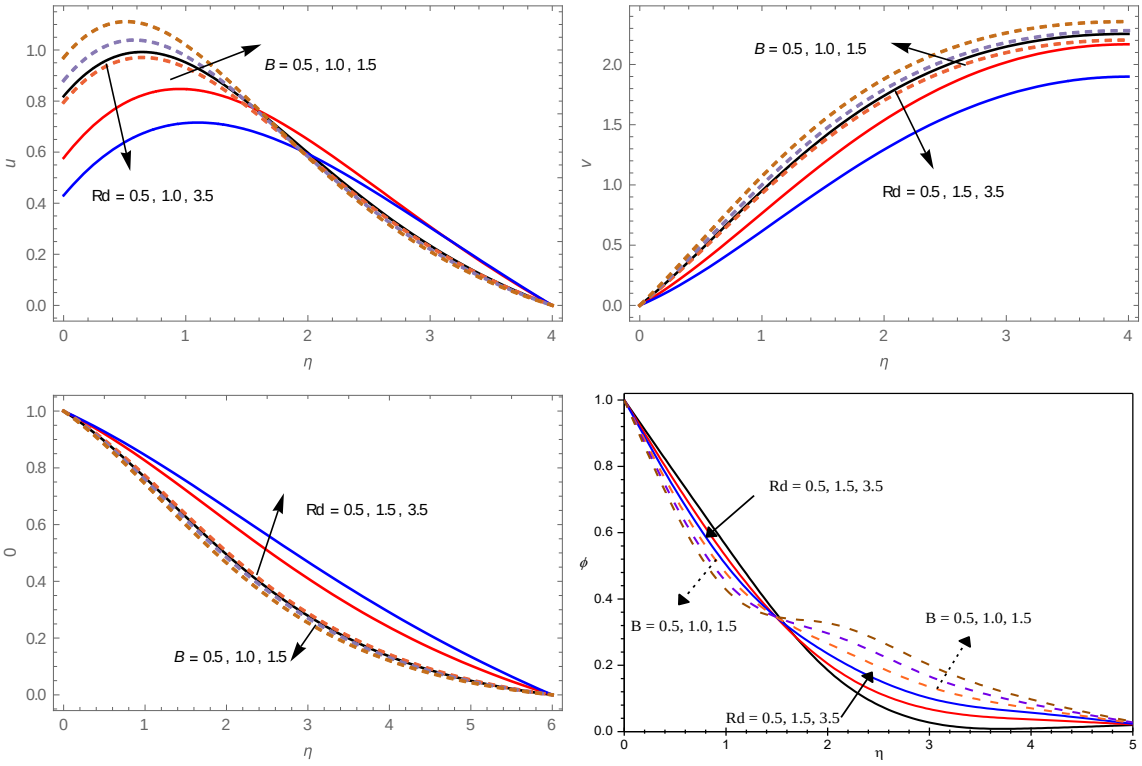

Fig.5 : Variation of [a].axial velocity(u), [b].Secondary Velocity(v), [c].Temperature(θ), [d].Nanoconcentration(ϕ) with Rd and B

Ra=2,M=0.5,K=0.2,N=0.5,Nb=0.1,Nt=0.1,Q=0.5,

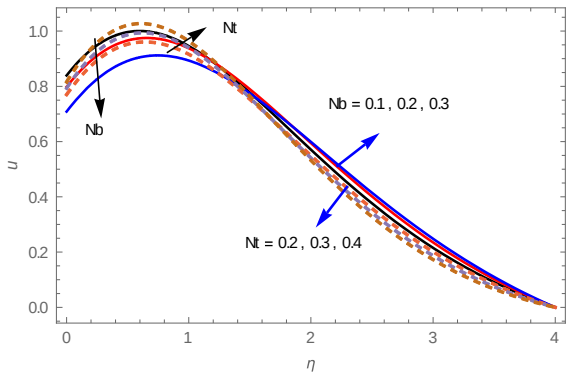

γ=0.2,E1=0.1,δ=0.1,a=0.1,ξ=π/4,Le=1,n=1

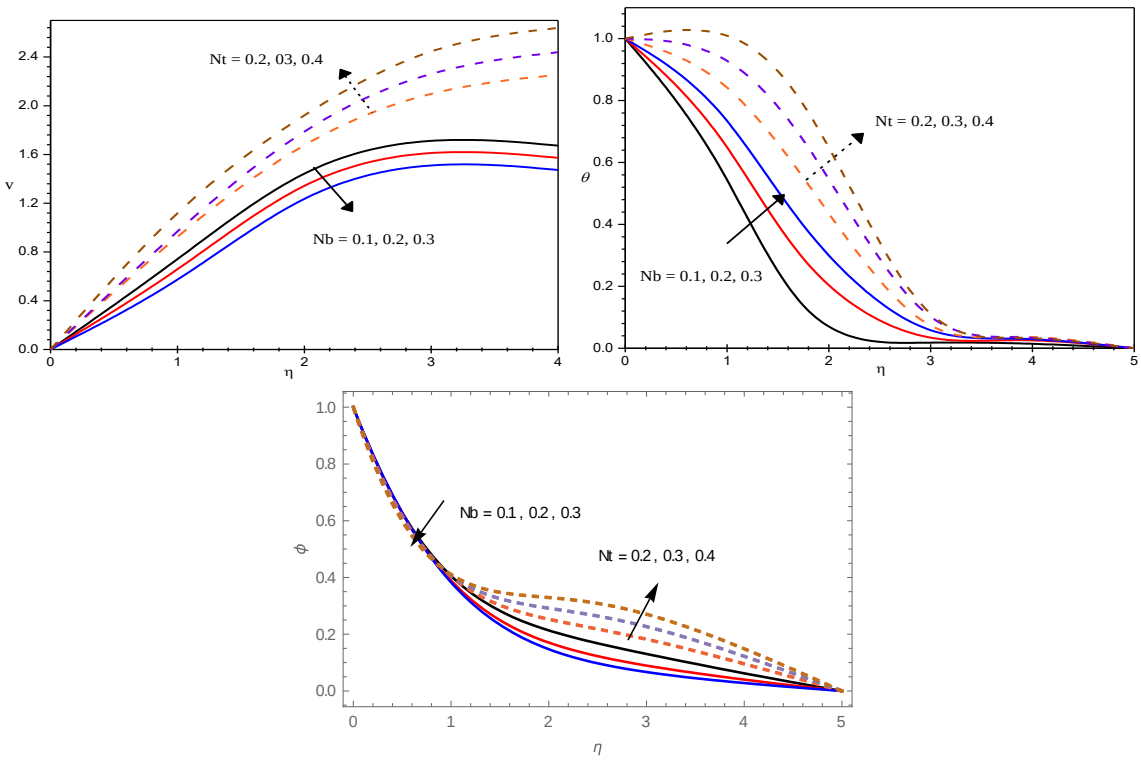

Fig.6: Variation of [a].axial velocity(u), [b].Secondary Velocity(v), [c].Temperature(θ), [d].Nanoconcentration(ϕ) with Nb and Nt

Ra=2,M=0.5,K=0.2,N=0.5,Rd=0.5,B=0.2,Q=0.5, γ=0.2,E1=0.1,δ=0.1,a=0.1,ξ=π/4,Le=1,n=1

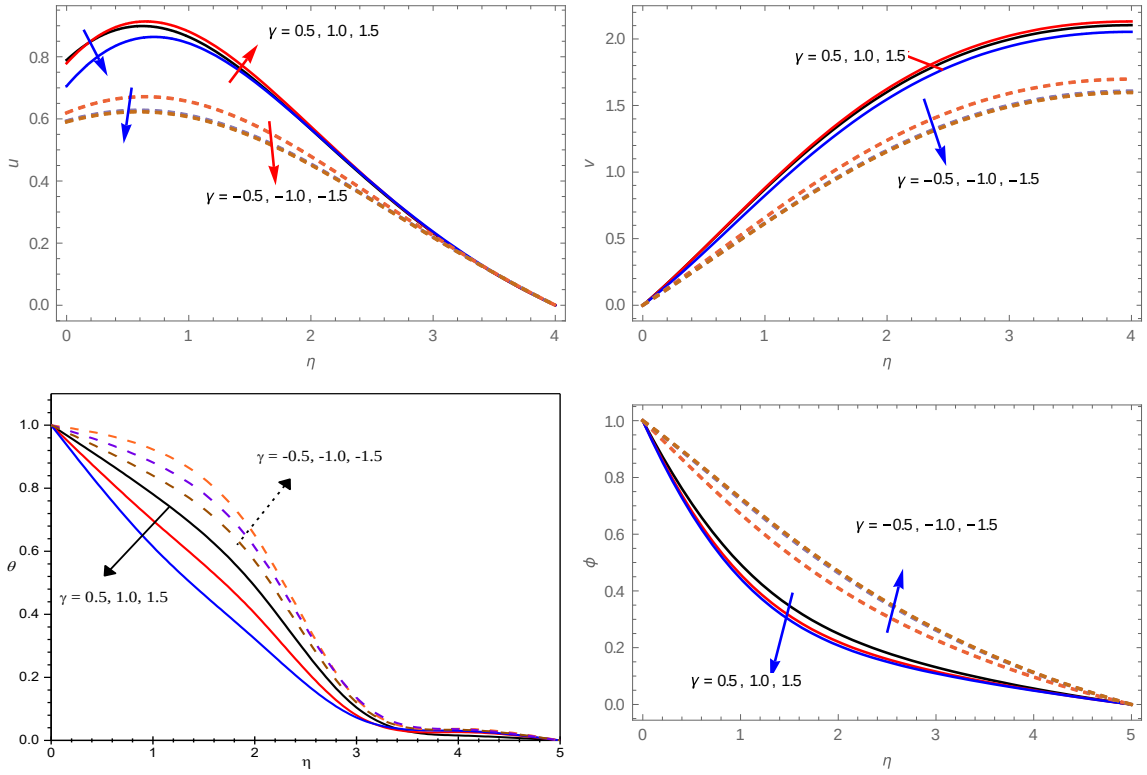

Fig.7: Variation of [a].axial velocity(u), [b].Secondary Velocity(v), [c].Temperature(θ), [d].Nanoconcentration(ϕ) with γ

Ra=2,M=0.5,K=0.2,N=0.5,Rd=0.5,B=0.2,Nb=0.1,Nt=0.1,
Q=0.5,E1=0.1,δ=0.1,a=0.1,ξ=π/4,Le=1,n=1

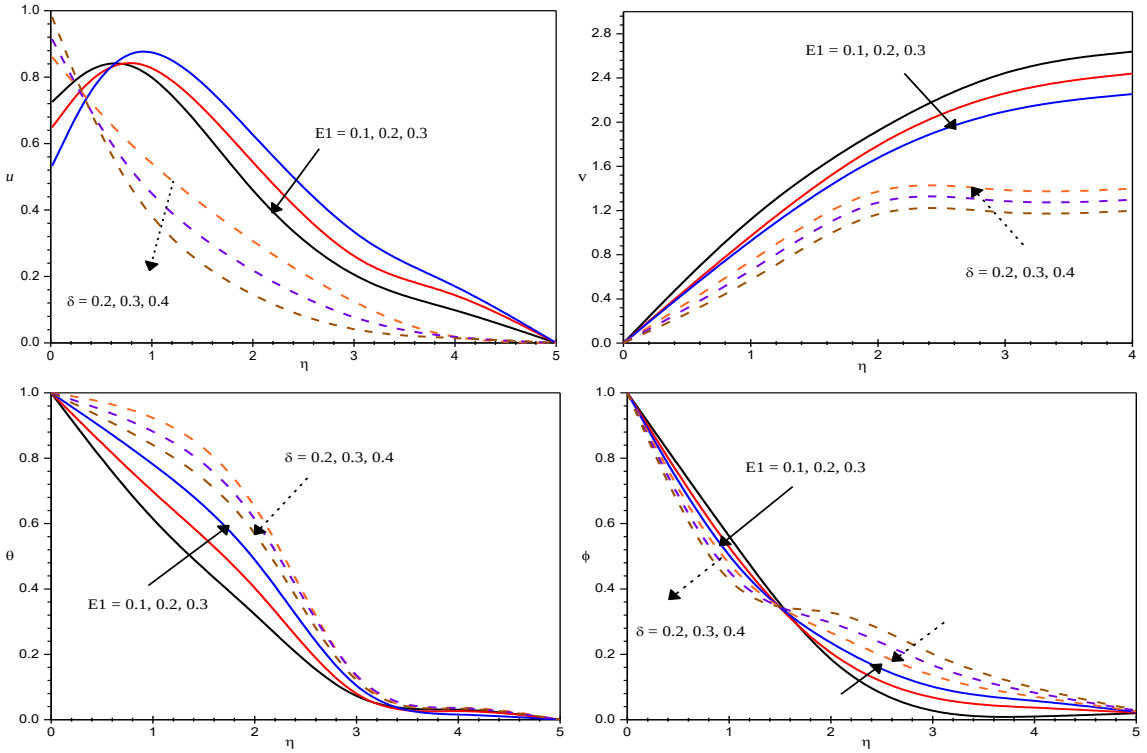

Fig.8 : Variation of [a].axial velocity(u), [b].Secondary Velocity(v), [c].Temperature(θ), [d].Nanoconcentration(ϕ) with E1 and δ

Ra=2,M=0.5,K=0.2,N=0.5,Rd=0.5,B=0.2,Q=0.5, γ=0.2,

Nb=0.1,Nt=0.1,a=0.1,ξ=π/4,Le=1,n=1

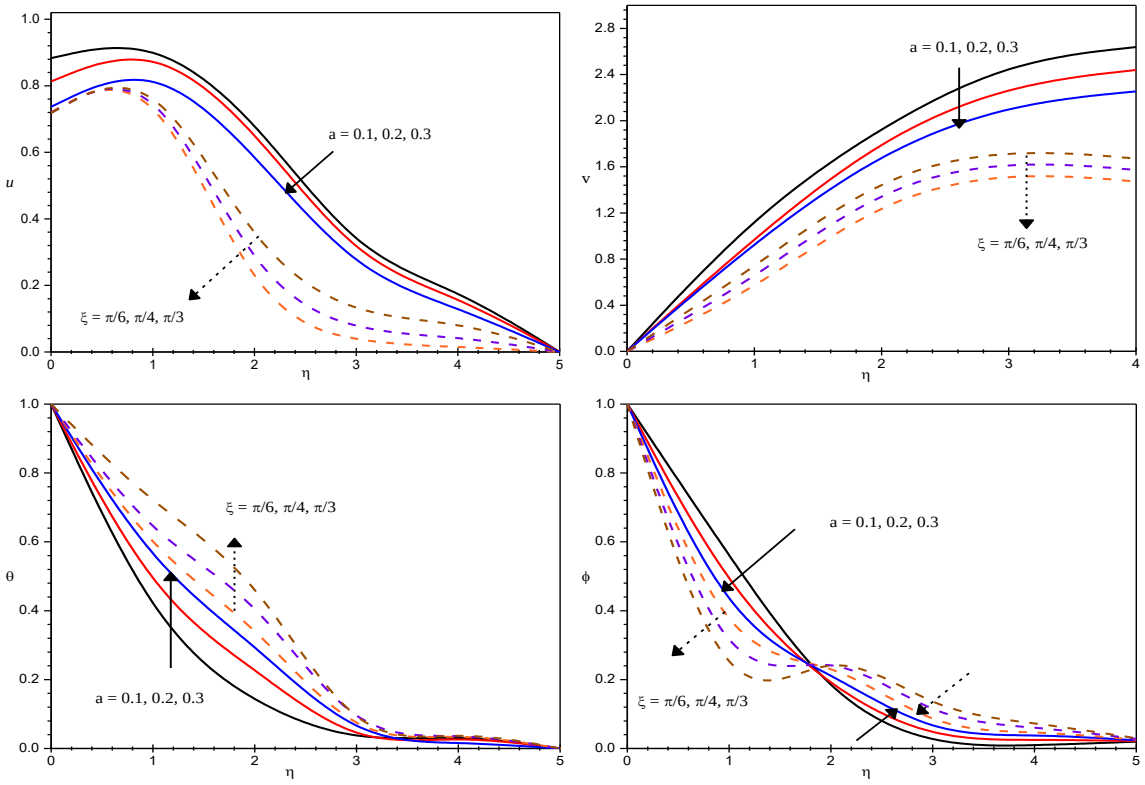

Fig.9 : Variation of [a].axial velocity(u), [b].Secondary Velocity(v), [c].Temperature(θ), [d].Nanoconcentration(ϕ) with a and ξ

Ra=2,M=0.5,K=0.2,N=0.5,Rd=0.5,B=0.2,Q=0.5, γ=0.2,
Nb=0.1,Nt=0.1,E1=0.1,δ=0.1,Le=1,n=1

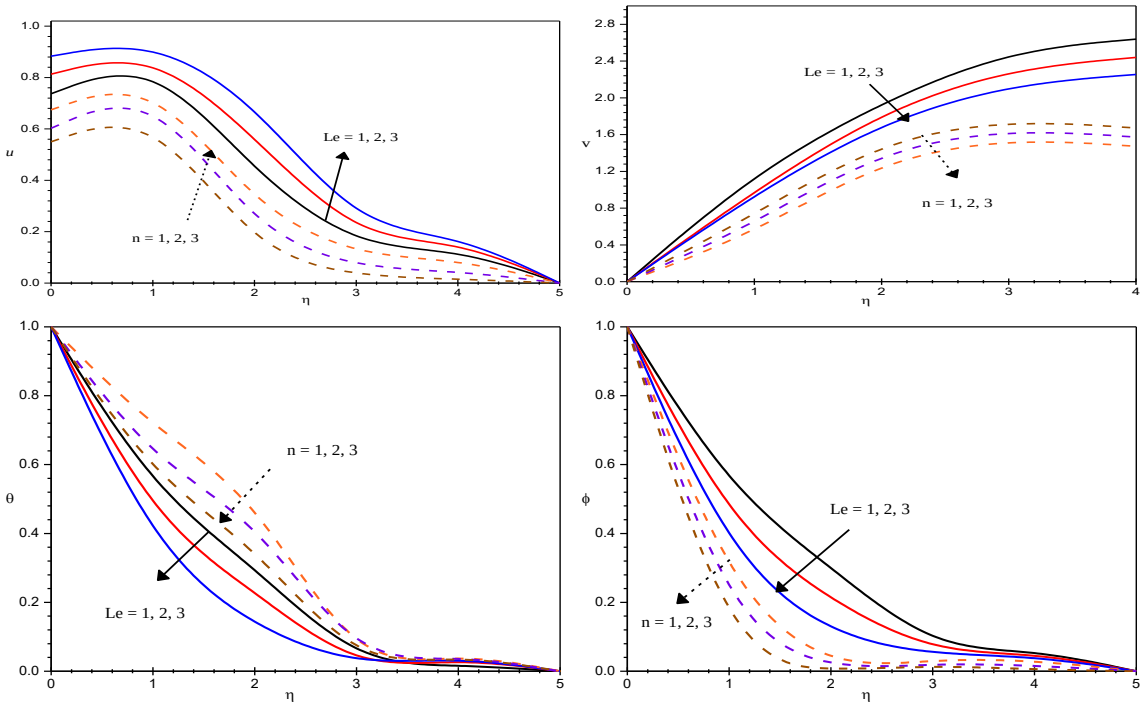

Fig.10 : Variation of [a].axial velocity(u), [b].Secondary Velocity(v), [c].Temperature(θ), [d].Nanoconcentration(ϕ) with Le and n

Ra=2,M=0.5,K=0.2,N=0.5,Rd=0.5,B=0.2,Q=0.5,Nb=0.1,

Nt=0.1,γ=0.2,E1=0.1,δ=0.1,a=0.1,ξ=π/4,

Table - 2

Skin Friction ($Cf_{x,y}$), Nusslet number (Nu) and Sherwood Number (Sh) at η = 0

Parameter		Cfx(0)	Cfy(0)	Nu(0)	Sh(0)	**Parameter**		Cfx(0)	Cfy(0)	Nu(0)	Sh(0)
Ra	2	0.574674	0.818901	0.178038	0.900953	Nt	0.1	0.635377	0.635377	0.160898	0.971442
	4	0.539544	1.28077	0.265445	0.915147		0.2	0.686285	0.686285	0.157784	1.016534
	6	0.477361	1.61492	0.317748	0.926959		0.3	0.738931	0.738931	0.154865	1.063754
M	0.5	0.559369	0.547308	0.114121	0.893788	a	0.1	0.574674	0.818901	0.178038	0.900953
	1.0	0.542411	0.426486	0.080844	0.890855		0.2	0.562286	0.803994	0.176837	0.893468
	1.5	0.523529	0.330452	0.051562	0.888547		0.3	0.543756	0.737189	0.165238	0.881098
K	0.2	0.574674	0.818901	0.178038	0.900953	ξ	π/6	0.570802	0.721622	0.156929	0.897217
	0.4	0.571644	0.611303	0.130721	0.895422		π/4	0.574248	0.719628	0.155848	0.899281
	0.6	0.552927	0.435724	0.084236	0.891087		π/3	0.575983	0.718625	0.155303	0.900322
N	0.5	0.686666	0.604942	0.142765	0.894166	γ	0.5	0.364202	0.789341	0.154903	0.917656
	1.0	0.800078	0.487455	0.128837	0.889844		1.0	0.431972	0.779115	0.158617	0.734843
	1.5	0.912725	0.367839	0.114553	0.885235		1.5	0.464755	0.705216	0.159493	0.705126
B	0.2	0.580088	0.795213	0.170956	0.900807		-0.5	0.158449	0.619631	0.086045	0.335991
	0.4	0.584007	0.880466	0.186444	0.903776		-1.0	0.112655	0.593437	0.070128	0.257108
	0.6	0.586766	0.970204	0.201617	0.906934		-1.5	0.107883	0.590211	0.068222	0.248368
Rd	0.5	0.574674	0.818901	0.178038	0.900953	E1	0.1	0.593464	0.820896	0.179737	0.921911
	1.5	0.617917	0.576993	0.142056	0.873443		0.2	0.587821	0.799507	0.174799	0.915465
	3.5	0.673501	0.430334	0.131988	0.845688		0.3	0.580612	0.721625	0.157255	0.908069
Q	0.5	0.574674	0.818901	0.178038	0.900953	δ	0.2	0.598194	0.723494	0.158615	0.928702
	1.0	0.769571	0.772812	0.109529	0.951554		0.3	0.619178	0.726542	0.160369	0.953462
	1.5	0.861159	0.679224	0.054088	0.977547		0.4	0.639804	0.728994	0.162042	0.977692
	-0.5	-0.199174	0.860678	0.425734	0.682189	Le	1	0.359734	0.808552	0.152524	0.648847
	-1.0	-0.530719	0.914833	0.538589	0.585103		2	0.574526	0.798048	0.173568	0.900367
	-1.5	-0.795252	0.951735	0.627411	0.505504		3	0.737269	0.737326	0.174272	1.099012
	0.1	0.573487	0.573487	0.185483	0.915573	n	1	0.542517	0.716538	0.153683	0.862432
	0.2	0.574526	0.574526	0.173568	0.900367		2	0.546314	0.717069	0.154033	0.866979
	0.3	0.582382	0.582382	0.145515	0.885601		3	0.550098	0.717594	0.154379	0.871506

7. References:

1. Abd El-Aziz, M., Flow and heat transfer over an unsteady stretching surface with Hall effect, Meccanica 45, 97-109 (2010).
2. Abo-Eldahab, E. M., Abd El Aziz, M., Hall and ion-slip effect on MHD free convective heat generating flow past a semi-infinite vertical flat plate, Phs. Scripta 61 (2000) 344.
3. Abo-Eldahab, E. M., Salem, A. M., Hall effects on MHD free convection flow of a non- Newtonian power-law fluid at a stretching surface, Int. Commun. Heat Mass 31(3), 343- 354 (2004)
4. Ali, F. M., Nazar, R., Arifin, N. M., and Pop, I., Effect of Hall current on MHD mixed convection boundary layer flow over a stretched vertical flat plate, Meccanica 46, 1103- 1112 (2011).
5. Alshomrani AS, Zaka Ullah M, Capizzano SS, Khan WA, Khan M. Interpretation of chemical reactions and activation energy for unsteady 3D flow of Eyring–Powell magneto涣nanofluid. Arabian J Sci Eng. 2019;44: 579-589.
6. Animasaun IL. Casson uid ow with variable viscosity and thermal conductivity along exponentially stretching sheet embedded in a thermally strati_ed medium with exponentially heat generation. J of Heat and Mass tran Res. 2015;2:63-78.

7. Azama M, Xu T, Shakoor A, Khan M. Effects of Arrhenius activation energy in development of covalent bonding in axisymmetric flow of radiative洽cross nanofluid. Int Commun Heat Mass Transfer. 2020;133: 10454.
8. Bandita P. E_ects of variable viscosity and thermal conductivity on the unsteady mhd slip flow of micropolar fluid over a vertical plate. Intern J of Comp Appl Tech and Res. 2017;6(7):293-298.
9. BejanA and KhairK.R: Heat and mass transfer by natural convection in a porous medium, International journal of Heat and Mass transferV.28(5)pp.909-918(1985)
10. Brewester M.Q : Thermal radiative transfer and properties. John Wiley & Sons. Inc. New York (1992).
11. Buongiorno, J., Convective transport in nanofluids, J. Heat Transfer 128 (2006) 240 – 250.
12. Ching-Yang Cheng : Double diffusive natural convection along an inclined wavy surface in a porous medium. Int. Comm. Heat and Mass transfer V.37 pp. 1471-1476 (2010).
13. Choi, S.U.S., Enhancing thermal conductivity of fluids with nanoparticles, Developments and Applications of Non-Newtonian Flows, FED-vol. 231/MD-vol. 66, 1995, pp. 99-105.
14. DeshikacharK.S and Ramachandra RaoA:Effect of a magnetic field on the flow and blood oxygenation in channel of variables cross section Int. J. Engg. Sci V.23p. 1121(1985)
15. Devi SPA, Prakash M. Temperature-dependent viscosity and thermal conductivity e_ects on hydromagnetic flow over a slendering stretching sheet. J of Nig Math Soc. 2015;34:318-330.
16. Dulal P, Hiranmony M. E_ects of temperature-dependent viscosity and variable thermal conductivity on mhd non-Darcy mixed convective di_usion of species over a stretching sheet. J of Egy Math Soc. 2014;22:123-133.
17. Eastman, J. A., Choi, S. U. S., Li, S., Thompson, L. J., and Lee, S., Enhanced thermal conductivity through the development of nanofluids, in: Nanophase and Nanocomposite Materials II, eds. S. Komarneni, J. C. Parker and H. J. Wollenberger, pp. 3 – 11 (1997), Materials Research Society, Pittsburgh.
18. Eastman, J. A., Choi, S. U. S., Li, S., Yu, W., Thompson, L. J., Anomalously increased effective thermal conductivity of ethylene glycol – based nanofluids containing copper nanoparticles, Appl. Phys. Lett., 78(6) : (2001) 718 – 720.
19. Gireesha B.J., M. Archana, B. Mahanthesh, Prasannakumara B.C., "Exploration of activationenergy and binary chemical reaction effects on nano Casson fluid flow with thermal and exponentialspace-based heat source", Multidiscipline Modeling in Materials and Structures, 15 : 1, 227-245, 2019
20. Gogula Sandhya, Ganganapalli Sarojamma, Panyam Venkata Satya Narayana, Bhumavarapu Venkateswarlu : Buoyancy forces and activation energy on the MHD radiative flow over an exponentially stretching sheet with second-order slip, Heat Transfer. 2021;50:784–800, DOI: 10.1002/htj.21904, wileyonlinelibrary.com/ journal/htj

21. Gopal CH, Bandita P. E_ects of variable viscosity and thermal conductivity on magnetohydrodynamics free convection flow of a micropolar fluid past a stretching plate through porous medium with radiation, heat generation and joule dissipation. Tur J of Phy. 2016;40:40-51.
22. Gopal CH, Jadav K. E_ects of variable viscosity and thermal conductivity on magnetohydrodynamics free convection dusty uid along a vertical porous plate with heat generation. Tur J of Phy. 2016;40:52-68.
23. Goren S.L. : On free convection in water at 4^{o}C. Chem. Engg. Sci. V.21 p.515 (1966)
24. Gorla, R. S. R. O., and Chamkha, A., Natural convective boundary layer flow over a horizontal plate embedded in a porous medium saturated with a nanofluid, Journal of Modern Physics, vol. 2, pp. 62 – 71, 2011.
25. Hamad, M. A. A., Ferdows, M., Similarity solution of boundary layer stagnation – point flow towards a heated porous stretching sheet saturated with a nanofluid with heat absorption/generation and suction/blowing: a lie group analysis. Commun Nonlinear Sci Numer Simulat 2011, 17(1) : 132 – 140.
26. Hamad, M.A., Pop, I., Ismail, A.I., Magnetic field effects on convection flow of a nanofluid past a vertical semi-infinite flat plate, Non-Linear Analysis: Real World Applications, vol.12, pp.1338-1346, 2011.
27. Hayat T, Khan SA, Khan MI, Alsaedi A. Theoretical investigation of Ree–Eyring nanofluid flow with entropy optimization and Arrhenius activation energy between two rotating disks. Comput Methods Programs Biomed. 2019;177:57-68.
28. Horuz E, Bozkurt H, Karatas H, Maskan M. Microwave逸conventional drying characteristics of red pepper: modeling, temperature profile, diffusivity and activation Energy. J Agric Sci Technol. 2020;22(2):425逸437.
29. Hossain M.A. Molla M.M. Yaa L.S. : Natural convective flow along a vertical wavy surface temperature in the presence of heat generation/ absorption Int. J. Thermal Science 43 pp157-163 (2004).
30. Ijaj Khan M, Sohail A, Khan, Hayat T, Imran Khan M and Alsaedi A : Arrchenius activation energy impact in binary chemically reactive flow of TiO_2-Cu-H2O hybird nanomaterial, International Journal of Chemical Reactor Engineering, (2018), DOI:10.1515/ijcre-2018-0183.
31. Ijaz M, Ayub M, Khan H. Entropy generation and activation energy mechanism in nonlinear radiative flow of Sisko nanofluid: rotating disk. Heliyon. 2019;5:e01863.
32. Isaac LA, Anselm OO. E_ects of variable viscosity, dufour, soret and thermal conductivity on free convective heat and mass transfer of non-Darcian flow past porous at surface. Amer J of Comp Math 2014;4:357-365.
33. Jadav K, Hazarika GC. E_ects of variable viscosity and thermal conductivity on mhd free convection flow of dusty fluid along a vertical stretching sheet with heat generation. Intern Res J of Eng and Tech. 2016;3(2):1029-1038.
34. Kareem RA, Salawu SO. Variable viscosity and thermal conductivity e_ects of soret and dufour on inclined magnetic _eld in non-Darcy permeable medium with dissipation. Brit J of Math and Comp Sci. 2017;22(3):1-12.

35. Keblinski, P., Phillpot, S. R., Choi, S. U. S., and Eastman, J. A., Mechanisms of heat flow in suspensions of nano – sized particles (nanofluids), Int. J. Heat and Mass Trans, 45(4), 855 - 863 (2002).
36. Khan M.I.T, Hayat M, Khan I, and Alsaedi A: Activatio Energy impact in Nonlinear Radiative Stagnation Point Flow of Cross Nanofluid, Int.Communiations Heat Massachusetts Transfer, V.91, pp.216-224, (2018)
37. Khan U, Zaib A, Khan Ilyas, Nisar KS. Activation energy on MHD flow of titanium alloy (Ti 6 Al4V) nano-particle along with a cross flow and streamwise direction with binary chemical reaction and non逸linear radiation: dual solutions. J Mater Res Technol. 2020;9(1):188-199.
38. Khan, WA, Pop, I, Boundary-layer flow of a nanofluid past a stretching sheet. Int. J Heat Mass Transf 53 (2010) 24772483
39. Kleinstreue, C., J. Li and J. Koo, Microfluidics of nano-drug delivery, Int. J. Heat and Mass Transf. 51(23), 5590-5597 (2008).
40. Kuznetsov, A. V., Nield, D. A., Natural convective boundary-layer flow of ananofluid past avertical plate, Int. J. Therm. Sci. 49 (2010) 243 – 247.
41. LaiF.C and KulackiF.A:International Journal of Heat and Mass transfer V.33 (5) pp.1028-1031(1990)
42. Leela Kumari S.N and Sarojamma G : Transient hydromagnetic convective heat and mass transfer flow of a chemically reacting viscous fluid in a vertical wavy channel with oscillatory flux. Journal of Pure and Applied Physics V.23 No.4 pp.601-611 (2011).
43. Makinde O.D., Mabood F, Khan W.A., Tshehla M.S. : MHD flow of a variable viscosity nanofluid over a radially stretching convective surface with radiative heat, Journal of Molecular Liquids, 219, (2016), pp.624-630, www.elsevier.com/ locate/molliq, http://dx.doi.org/10.1016/j.molliq.2016.03.078
44. Makinde, O. D., Aziz, A., Boundary layer flow of a nanofluid past a stretching sheet with convective boundary condition, Int. J. of Therm. Sci. 50 (2011) 1326 – 1332.
45. Mallikarjuna B : Convective heat and mass transfer in viscous fluid flow over a porous medium Ph.D. thesis JNTUA Ananthapuramu June 2014.
46. Manjulatha V : Heat and mass transfer in fluid flows through porous media in an aligned magnetic field. Ph.D Thesis S.V.University Tirupati India (2013).
47. Md Faisal Md B, Kumar R, Ismail AI Md, et al. Exploration of thermal diffusion and diffusion thermal effects on the motion of temperature dependent viscous fluid conveying microorganism. Arabian J Sci Eng. 2019;44:8023逸8033.
48. Minsta, H. A., Roy, G., Nguyen, C. T., Doucet, D., New temperature dependent thermal conductivity data for water – based nanofluids, Int. J. Thermal Sci. 48 : (2009) 363 – 371.
49. Mohamed Abd El-Aziz, Effects of Hall current on the flow and heat transfer of a nanofluid over a stretching sheet with partial slip, International Journal of Modern Physics C, Vol. 24, No. 7 (2013) 1350044.
50. Nadeem, S., Lee, C., Boundary layer flow of a nanofluid over an exponentially stretching surface. Nanoscale Res Lett 2012, 7:94.

51. Ramakrishna G.N., and Satyanarayana K : “Effect of heat sources and thermal radiation on convective heat transfer flow past a vertical wavy wall with variable viscosity and thermal conductivity”, International Journal of Mathematical Archieve (IJMA), Vol.10, No.11, pp:15-25, (2019). ISSN 2229-5046, web: www.ijma.info.
52. Rana, P., Bhargava, R., Flow and heat transfer of a nanofluid over a nonlinearly stretching sheet: A numerical study, Communications in Nonlinear Science and Numerical Simulation, 2011.
53. Rao D.R.V, Krishna D.V and Debnath L: Combined effect of free and forced convection on Mhd flow in a rotating porous channelInt.J.Maths and Math.SciV.5pp.165-182(1982)
54. Rees D.A.S Pop I : Free convection induced by a vertical wavy surface with uniform heat flux in a porous medium. ASME J. Heat Transfer V.117 pp. 547-550 (1995).
55. Saida Rashid, Tasawar Hayat, Sumaira Qayyum, Muhammad Ayub, Ahmed Alsaedi, "Threedimensionalrotating Darcy–Forchheimer flow with activation energy", Int. Journal of Numerical Methods for Heat & Fluid Flow, 29 : 3, 935-948, 2019
56. Sarojamma G, Vijaya Lakshmi R, Satya Narayana PV, Animasaun IL. Exploration of the significance of autocatalytic chemical reaction and Cattaneo–Christov heat flux on the dynamics of a micropolar fluid. J Appl Comput Mech. 2020;6(1):77逸89.
57. Shafiq Ahmad and Sohail Nadeem : Analysis of activatio energy and its impact of hybrid nanofluid in the presence of Hall and ion slip currents, Applied Nanoscience (Springer), (2020), https://doi.org/10.1007/s13204-020-01334-w
58. Shalini B.V Rathish Kumar : Influence of variable heat flux on natural convection along a corrugated wall in porous media. Comm. Nonlinear Sci. Num. Simulation V.12 pp.1454-1463 (2007).
59. Shamshuddin MD, Satya Narayana PV. Combined effect of viscous dissipation and Joule heating on MHD flow past a Riga plate with Cattaneo–Christov heat flux. Indian J Phys. 2020;94:1385逸1394.
60. Singh V, Shweta A. Flow and heat transfer of maxwell fluid with variable viscosity and thermal conductivity over an exponentially stretching sheet. Amer J of Fluid Dyn. 2013;3(4):87-95.
61. Sreenivasulu P, Poornima T, Bhaskar R. Variable thermal conductivity influence on hydromagnetic flow past a stretching cylinder in a thermally strati_ed medium with heat source/sink. Fron in Heat and Mass Trans. 2017;9(20):1-7.
62. Sreeramachandra MurthyA:Buoyancy induced hydromagnetic flows through a porous medium-A study Ph.D thesis S.K.University Anantapur A.P India (1992)
63. Sultan F, Khan WA, Ali M, Shahzad M, Irfan M, Khan M. Theoretical aspects of thermophoresis and Brownian motion for three-dimensional flow of the cross fluid with activation energy. Pramana. 2019;92:21.Article number: 21.
64. Srinivasa Reddy,B and Ranganatha Reddy,P:Convective heat and mass transfer flow of nanofluid past a vertical wavy wall with thermal radiation and chemical reaction,Pensee Journal,vol.51,Issue.3,Issn No.00314773,pp.1534-1558(2021)
65. Vajravelu K and DebnathL:Non-linear study of convective heat transfer and fluid flows induced by traveling thermal wavesActa MechV.59pp.233-249(1986)

66. Vajravelu K and Neyfeh A.H:Influence of wall waviness on friction and pressure drop in channels Int.J.Mech and Math.Sci.V.4N0.4pp.805-818(1981)
67. Vajravelu K and Sastry K.:Forced convective heat transfer in a viscous incompressible fluid confined between a long vertical wavy wall and parallel flat wall J. fluid. Mech, v.86(20p.365(1978)
68. Vajravelu K, Prasad KV, Chiu-on N. Unsteady convective boundary layer flow of a viscous fluid at a vertical surface with variable fluid properties. Nonl Analy: Real World Appl. 2013;14:455-464.
69. Vajravelu.K Hadjinicolaou.A : Heat transfer in a viscous fluid over a stretching sheet with viscous dissipation and internal heat generation Int. Comm. Heat Mass transfer 20 pp.417-430 (1993).
70. Vendabai K : Mathematical modelling of heat transfer in nanofluids, Ph.D. Thesis, Sri Padmavathi Mahila Visvavidyalayam, 2015.
71. Waqas M, Naz S, Hayat T, Alsaedi A. Numerical simulation for activation energy impact in Darcy–Forchheimer nanofluid flow by impermeable cylinder with thermal radiation. Appl Nanosci. 2019;9: 1173-1182.
72. Xiaohonh Su, Liancun Zheng, Hall effect on MHD flow and heat transfer of nanofluids over a stretching wedge in the presence of velocity slip and Joule heating, Cent. Eur. J. Phys. 11(12) . 2013.1694 – 1703.
73. Zeeshan A., Shehzad N., Ellahi R., “Analysis of activation energy in Couette-Poiseuille flow of nanofluid in the presence of chemical reaction and convective boundary conditions”, Results in Physics, 8 : 502–512, 2018.